

Supplemental information

**Intercellular extrachromosomal DNA copy-number
heterogeneity drives neuroblastoma
cell state diversity**

Maja C. Stöber, Rocío Chamorro González, Lotte Brückner, Thomas Conrad, Nadine Wittstruck, Annabell Szymansky, Angelika Eggert, Johannes H. Schulte, Richard P. Koche, Anton G. Henssen, Roland F. Schwarz, and Kerstin Haase

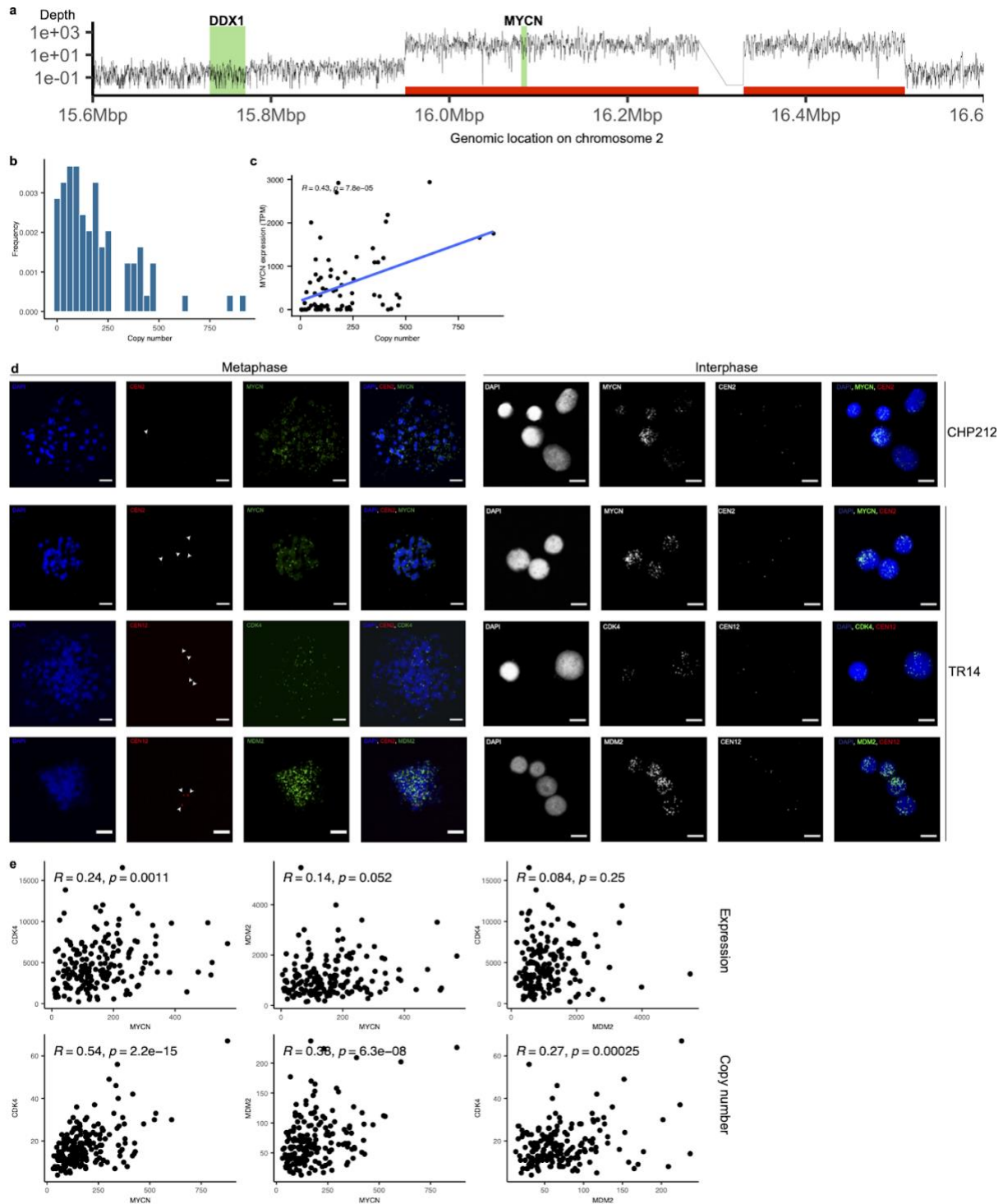


Figure S1: ecDNA copy number heterogeneity in neuroblastoma cell lines and patients, Related to Figure 1

a) Average genome coverage of selected region on chromosome 2 in ecDNA G&T-seq of patient, highlight ecDNA amplicon boundaries (red), DDX1 and MYCN gene location (green). b) Distribution of ecDNA amplicon copy number adapted from Ginkgo copy number profiles (500kb bin size) from single-cell whole genome sequencing for *MYCN* in patient. c) Correlation of gene expression and copy number of *MYCN* in

patient, Pearson correlation coefficient and p-value are given as inset. d) FISH images of metaphase spreads (left) and interphase spreads (right) of CHP212 and TR14 stained for nucleus (blue), for centromere of chromosome 2 or 12 (red) and MYCN, CDK4, MDM2(green). e) Pairwise correlation of amplified oncogenes *MYCN*, *CDK4* and *MDM2* in TR14 cells based on gene expression in TPM (top) and ecDNA amplicon copy number (bottom), Pearson correlation coefficient and p-value are given as inset.

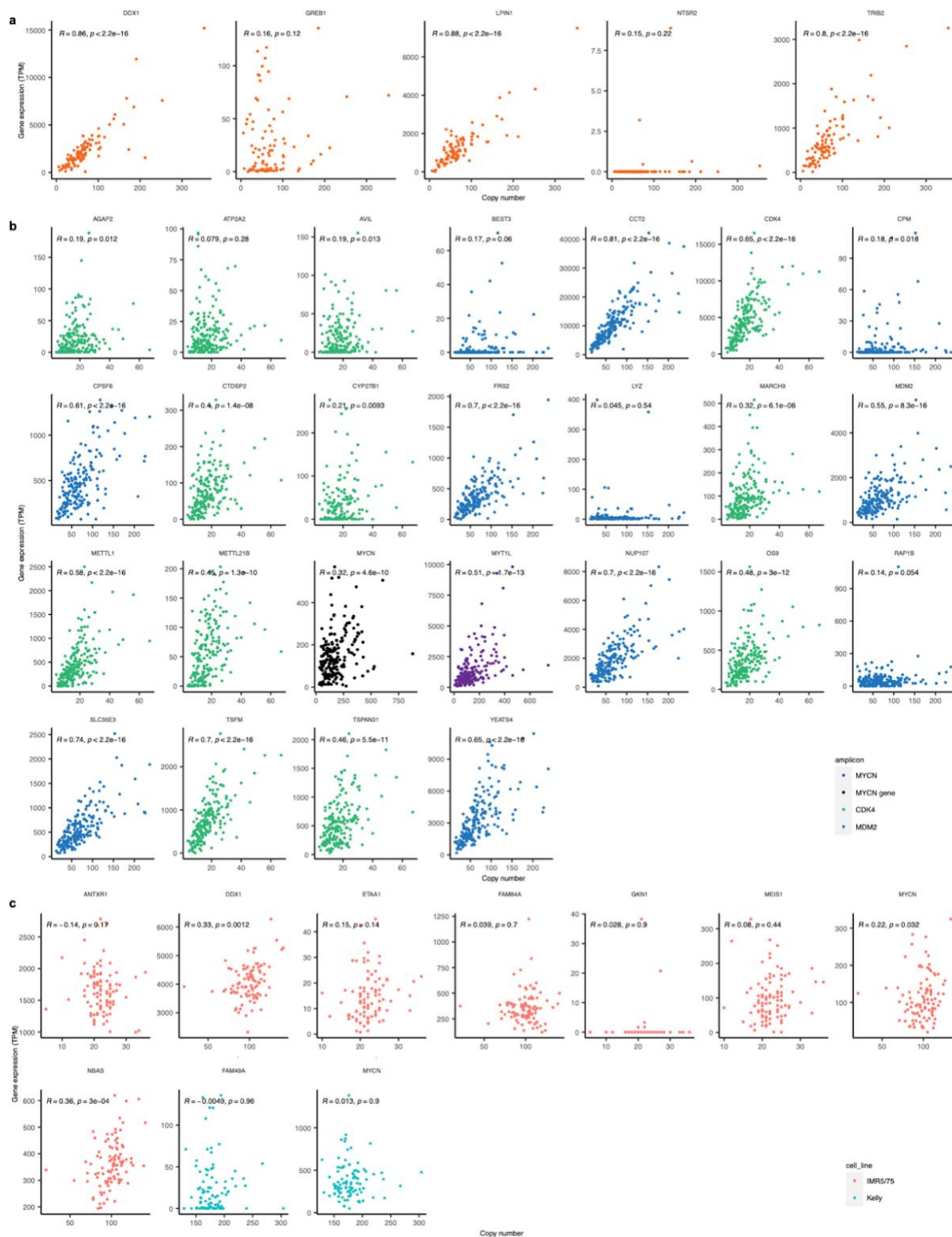


Figure S2: Correlation of ecDNA copy number and gene expression, Related to Figure 2

a) Correlation of gene expression and copy number of all genes on the *MYCN*-amplicon in CHP212, Pearson correlation coefficient and p-value are given as inset. b) Correlation of gene expression and copy

number of all genes on the *MYCN*-amplicon (purple), *CDK4*-amplicon (green), *MDM2*-amplicon (blue) in TR14, Pearson correlation coefficient and p-value are given as inset. c) Correlation of gene expression and copy number of all genes on the *MYCN*-amplicon in Kelly (blue) and IMR5/75 (red), Pearson correlation coefficient and p-value are given as inset.

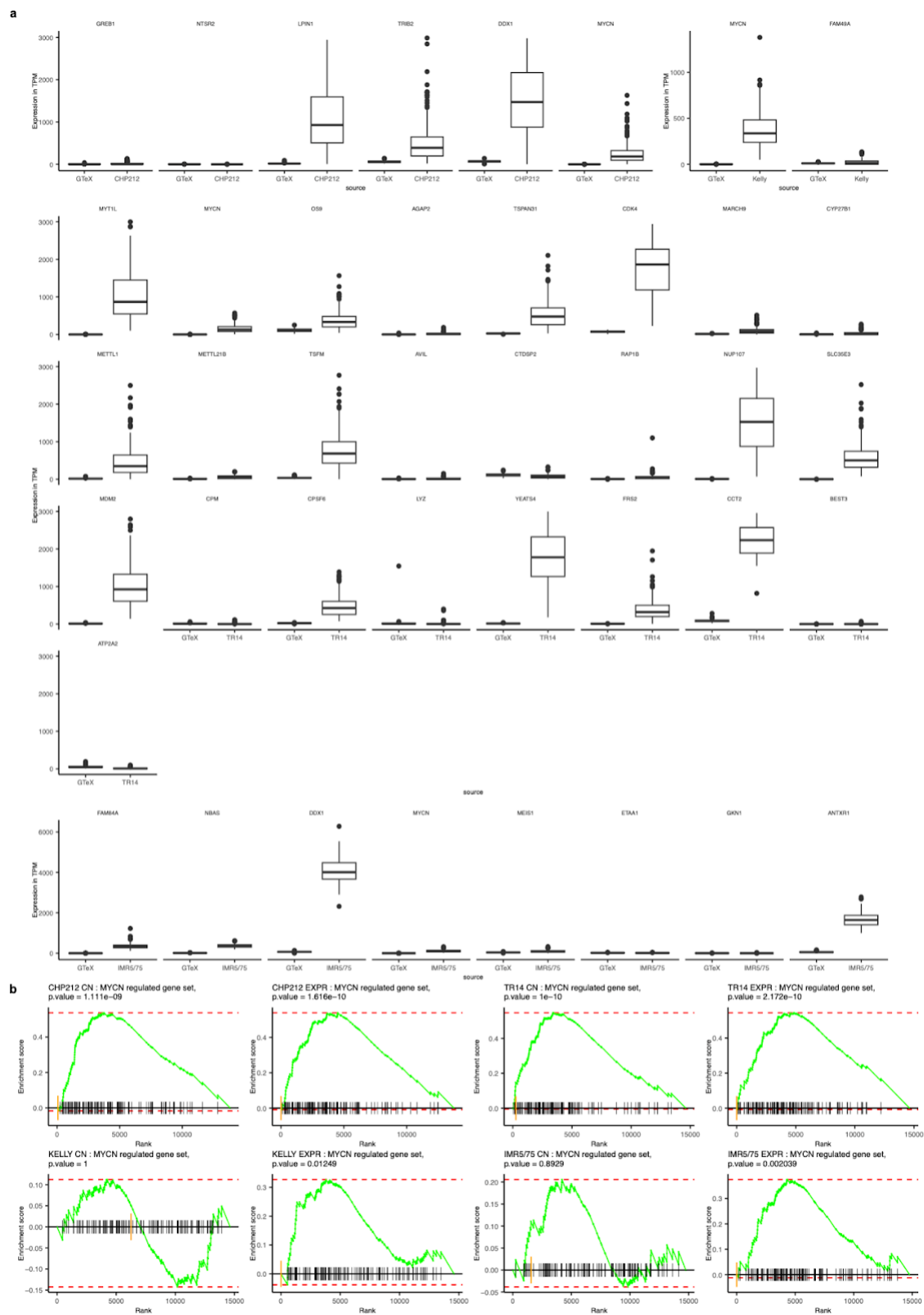


Figure S3: Functionality of amplified genes, Related to Figure 2

a) Boxplot of gene expression in TPM of amplicon genes in CHP212, TR14, IMR5/75 and Kelly cells compared to gene expression in normal adrenal gland cells. b) GSEA of *MYCN* target genes, genes decreasingly ordered by logarithmic fold change derived from differential gene expression analysis between *MYCN*-high and *MYCN*-low cells stratified by copy number (CN) or *MYCN* expression (EXPR) for CHP212, TR14, IMR5/75 and Kelly.

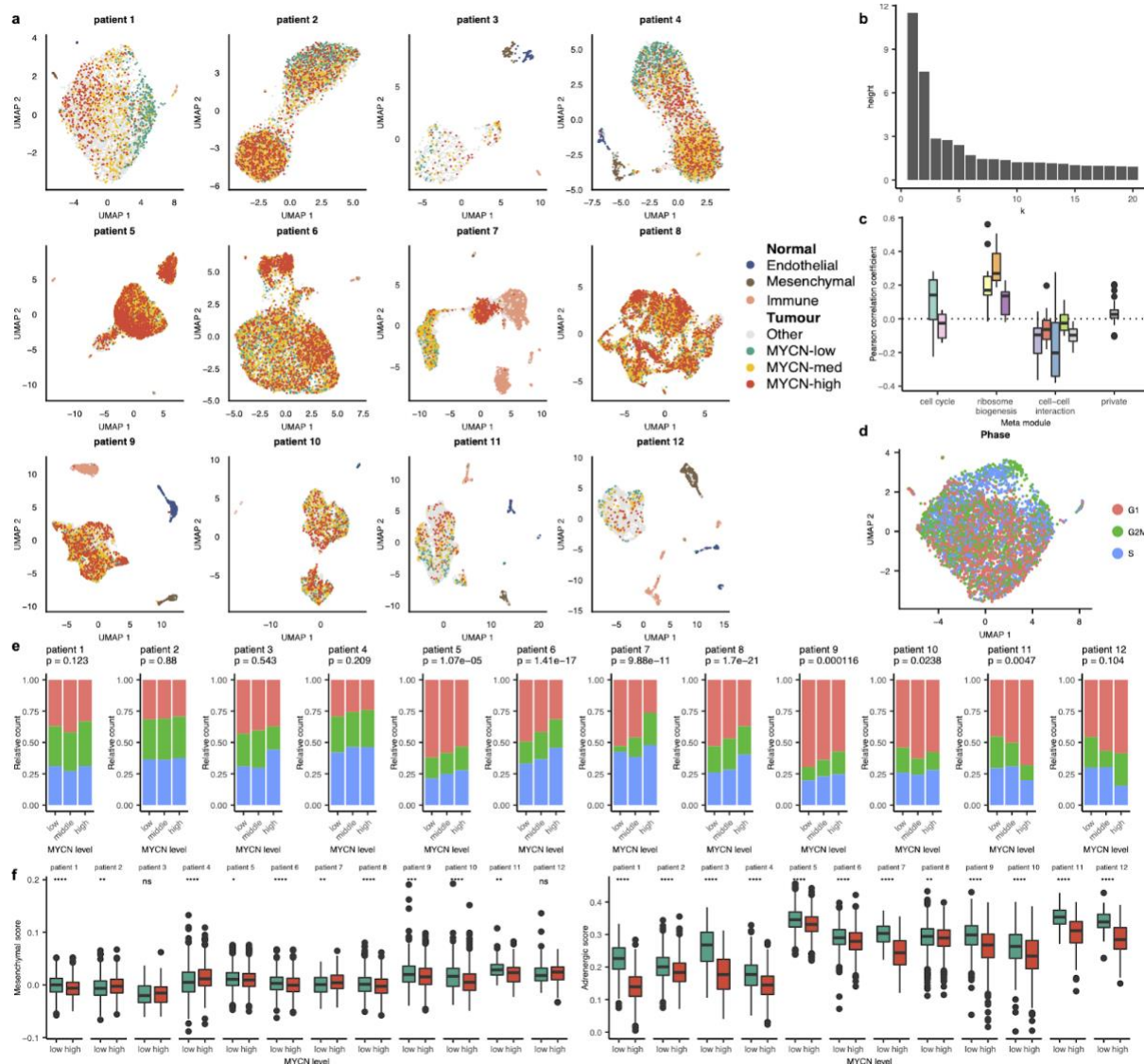


Figure S4: Intercellular tumour heterogeneity of 12 *MYCN*-amplified neuroblastoma patients, Related to Figure 3

a) Single-nuclei of 12 *MYCN*-amplified neuroblastoma patients were sequenced and grouped by cell type, including mesenchymal (brown), immune (orange), endothelial (blue) and tumour cells, which were grouped by low (green), intermediate (yellow) and high (red) *MYCN* expression. b) Barplot of heights in dendrogram from NMF correlation matrix. c) Boxplot of Pearson correlation coefficient between *MYCN* expression and submodule activity grouped by metamodule. d) UMAP of patient 1 coloured by cell cycle phase. e) Stacked barplot of cells with high, intermediate and low *MYCN* expression, coloured by cell cycle phase, Chi-square

p-value given as inset. f) Boxplot of mesenchymal and adrenergic score for each patient grouped by MYCN-high (red) and MYCN-low (green) cells, asterisks represent significance level of Wilcoxon test with ns: p-value (p) > 0.05, *: $p \leq 0.05$, **: $p \leq 0.01$, ***: $p \leq 0.001$, ****: $p \leq 0.0001$.

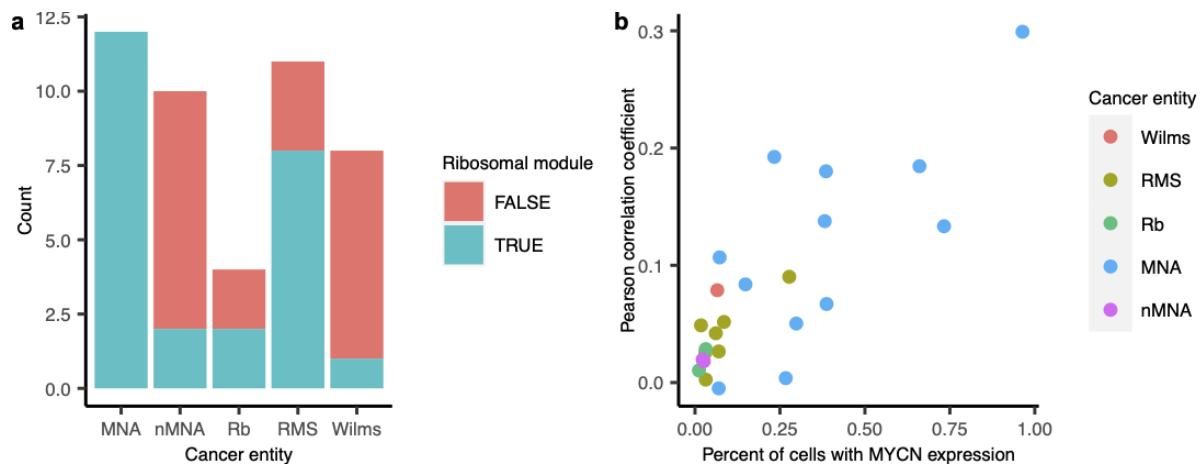


Figure S5: Ribosome biogenesis activity in paediatric cancer entities, Related to Figure 4

a) Number of samples where ribosome biogenesis was identified using NMF in MYCN-amplified neuroblastoma (MNA), non-MYCN-amplified neuroblastoma (nMNA), Retinoblastoma (Rb), Rhabdomyosarcoma (RMS) and Wilms tumour. b) Correlation between *MYCN* expression and ribosomal module activity per sample.